NACA RM No. L7K14

NACA

RESEARCH MEMORANDUM

FLIGHT TESTS TO DETERMINE THE EFFECT OF AIRFOIL SECTION PROFILE AND THICKNESS RATIO ON THE ZERO-LIFT DRAG OF LOW-ASPECT-RATIO WINGS AT SUPERSONIC SPEEDS

By

Ellis Katz

Langley Memorial Aeronautical Laboratory
Langley Field, Va.

NATIONAL ADVISORY COMMITTEE
FOR AERONAUTICS

WASHINGTON

February 9, 1948

NATIONAL ADVISORY COMMITTEE FOR AERONAUTICS

RESEARCH MEMORANDUM

FLIGHT TESTS TO DETERMINE THE EFFECT OF AIRFOIL SECTION PROFILE AND THICKNESS RATIO ON THE ZERO-LIFT DRAG OF LOW-ASPECT-RATIO WINGS AT SUPERSONIC SPEEDS

By Ellis Katz

SUMMARY

Flight tests of airplane-like model configurations have been conducted to determine the effect of airfoil section profile and thickness ratio on the zero-lift drag of low-aspect-ratio wings at supersonic speeds. Five rectangular wings of 1.5 aspect ratio having NACA 65-series airfoil sections of from 0.0912 to 0.0300 thickness ratio were compared to determine the effect of thickness ratio. Three 45° sweptback wings of 2.7 aspect ratio having circular-arc, diamond, and NACA 65-009 airfoil sections of equal thickness ratios were compared to determine the effect of section profile.

The results indicated that, for the round-nose NACA sections, a decrease of thickness ratio resulted in a marked reduction of wing drag which, however, was less than that indicated by the theoretical thickness-squared relation for pure supersonic flow. Almost half the drag reduction resulting from sweep was due to the decrease of the thickness ratio in the free-stream direction. For both the rectangular and 45° sweptback wings, the use of sharp-nose profiles resulted in greater drag than for the round-nose NACA 65-009 airfoil sections, though the effect of profile appeared very small for the swept plan form.

INTRODUCTION

As part of an NACA investigation to determine the zero-lift drag of airfoil surfaces at supersonic speeds, this report presents results of tests made to determine the effects of section thickness ratio and profile on the drag of low-aspect-ratio wings.

One of the means by which practical flight efficiencies might possibly be attained in the supersonic speed range is by the use of very thin airfoil section profiles. To determine the effect of section thickness on the zero-lift drag coefficient of rectangular wings, five configurations have been tested with rectangular wings of differing thickness ratios.

As a further means of reducing the drag of wings at supersonic speeds, sharp-nose airfoil sections have been investigated, as given in reference 1. Theoretical considerations indicate that sharp-nose profiles might show lower drag at supersonic speeds than conventional round-nose sections. At low supersonic Mach numbers, however, the theory fails in accuracy and results must be obtained by experiment. Reference 2 presented a comparison between a circular-arc and NACA 65-009 airfoil section for a rectangular plan form. This report extends the results of reference 2 to include comparisons between the diamond, circular-arc, and NACA 65-009 airfoil sections for a 45° sweptback plan form.

The wing drag presented in this report includes mutual interference effects between wing and body. The Mach number range from 0.95 to 1.3 corresponds to a Reynolds number range from approximately 5×10^6 to 9×10^6 depending on wing chord and Mach number.

SYMBOLS

A	aspect ratio (b/c)
b	wing span measured normal to plane of symmetry, feet
c	wing chord measured parallel to plane of symmetry, feet
$\frac{t}{c}$	section thickness ratio
t	section thickness, feet
Λ	angle of sweepback, degrees
C_{D_w}	wing-drag coefficient
C_{D_f}	viscous drag coefficient
C_{D_T}	total drag coefficient
M	Mach number
W	burned-out weight of test model, pounds
a	measured deceleration of test model, feet per second per second
g	acceleration of gravity (32.1740 ft/sec^2)
S	exposed wing plan-form area, square feet

[redacted]

ρ atmospheric density, slugs

V model velocity, feet per second

θ launching angle, degrees

MODELS AND TESTS

All test models were identical with the exception of the wings. Photographs of the configurations tested are shown as figures 1 and 2. The plan form of all wings was so located that the quarter-chord point of the mean geometric chord was 3.4 diameters rearward of the base of the nose. The wing surfaces were rotated 45° out of the plane of the tail fins. A Mk.7 aircraft rocket motor which develops approximately 2000 pounds thrust for 1 second was housed within the cylindrical body. Wood construction was used throughout.

Four configurations with rectangular wings of A = 1.5 and NACA 65-series airfoil sections were tested for the thickness-ratio investigation. Three of the configurations had wings with thickness ratios equivalent to the streamwise thickness ratios for the 34°, 45°, and 52° sweptback wings of reference 3. The test wings were actually of $\frac{t}{c}$ = 0.0746, 0.0639, and 0.0557; and the exposed plan-form area was 1.277 square feet. A fourth configuration was tested with 0.03 thickness ratio and exposed plan-form area of 1.389 square feet. For the section profile investigation, two configurations having 45° sweptback nontapered wings of 2.7 aspect ratio and 1.389 square feet exposed plan-form area were tested with 9-percent-thick diamond and circular-arc sections normal to the leading edge. Figure 3 presents the diamond and circular-arc profiles of 9-percent thickness in comparison with the NACA 65-009 airfoil section profile.

The experimental data were obtained by launching the model at an angle of 75° to the horizontal and determining its velocity along the nearly straight-line flight path. The velocity determination is made possible by a Doppler radar velocimeter located at the point of launching. The data were obtained from one test for the sweptback circular-arc winged configuration and two or more tests for the remaining configurations. The total drag coefficient values are derived from the formula

$$C_{D_T} = \frac{2W(a - g \sin \theta)}{g\rho SV^2}$$

The sine of the launching angle θ is assumed to be equal to 1.00, the resulting error being of the order of 0.5 percent and, hence, considered negligible. The basic data for each model of every configuration tested are plotted in figure 4 as C_{D_T} versus M. For each

configuration faired curves have been drawn through the basic data of figure 4, and these curves will be used as the basis of the following discussion.

RESULTS AND DISCUSSION

Thickness Ratio

Curves of C_{D_T} versus M for the rectangular winged configurations are shown in figure 5 for $\frac{t}{c} = 0.0756$, 0.0639, and 0.0557 for which S = 1.277 square feet, and in figure 6 for $\frac{t}{c} = 0.0912$ (reference 3) and 0.0300 for which S = 1.389 square feet. Also included in figures 5 and 6 is the curve for the wingless configuration of reference 4 which, however, is based on a wing area of 1.277 square feet in figure 5 and 1.389 square feet in figure 6. Other than being wingless, this configuration is similar to the configurations of this report. Figure 7 shows the variation of C_{D_W} with M for five values of thickness ratio.

C_{D_W} is the increment in drag coefficient that results from the addition of a wing to a wingless configuration. Although the wings of $\frac{t}{c} = 0.0912$ and 0.0300 were of a slightly different exposed area than the remaining test wings, the discrepancy is believed to have negligible effect on the comparative results. The curves show that thin wing sections are definitely superior to thick ones. The fact that the wings of $\frac{t}{c} = 0.0639$ and 0.0557 do not appear in the correct order for $M < 1.15$ is due perhaps to the inherently larger experimental inaccuracies near M = 1.0 rather than to aerodynamic phenomena.

The results of figure 7 are cross-plotted in figure 8 to show the variation of wing-drag coefficient with thickness ratio and thickness ratio squared at a Mach number of 1.20. The curves of figure 8 have been extrapolated to zero thickness ratio where the wing-drag coefficient is equal to the viscous drag coefficient C_{D_f}. A value of $C_{D_f} = 0.006$ has been obtained from reference 5 for an assumed turbulent boundary layer at the Reynolds number of the tests. For M = 1.2, the curves indicate a nearly linear variation of C_{D_W} with t/c throughout the test range from $\frac{t}{c} = 0.0912$ to 0.0300 although it might be expected that the variation becomes nonlinear at very low values of t/c as is suggested by the extrapolation. Reference 6 showed that the pressure drag coefficient of a wing in pure supersonic flow should theoretically vary as the square of its thickness ratio. Although the wings with NACA 65-series airfoil sections are not theoretically in a pure supersonic

flow field, owing to the rounded leading edges and detached nose waves, it is of interest to compare the experimental results for transonic flow with the linearized theory for supersonic flow. When plotted against $(t/c)^2$, the theoretical variation was a straight line which was made to pass through the experimental value of C_{D_W} at $\left(\frac{t}{c}\right)^2 = 0.00832$ and $C_{D_W} = C_{D_f} = 0.006$ at $\left(\frac{t}{c}\right)^2 = 0$. This theoretical variation is shown as a dashed line in figure 8 for comparison with the experimental variation. It is seen that the supersonic theory predicts a greater drag coefficient decrement due to a thickness ratio reduction of the 9-percent-thick section than is experimentally realized. It is possible that part or all of this difference between the experimental and theoretical variation may be due to the mutual interference effects mentioned previously.

The effect of sweepback Λ was reported in reference 3 where, for the purpose of the investigation, aspect ratio, exposed planform area, and airfoil section normal to the leading edge were held constant for various values of sweep. However, the decrement of C_{D_W} between the unswept and sweptback wings of reference 3 may be considered to be the end result of two independent effects: first, a reduction of the free-stream-direction thickness ratio of the rectangular wing to the ratio corresponding to the swept wing and, second, a shearing back of the reduced sections so that the leading edge is swept to the desired Λ. These steps are diagrammatically shown in figure 9. The results of reference 3 for $M = 1.2$ are plotted in figure 10 as the variation of C_{D_W} with the free-stream thickness ratio for wings having varying degrees of sweepback. Also replotted in figure 10 is the curve from figure 8 for $M = 1.2$ for which all wings were unswept. The lower curve shows the sum result of the two effects mentioned above. The first effect, that of the t/c reduction for the rectangular wing, is shown by the upper curve in figure 10 and is the result of the first effect alone. The difference between the curves denotes the magnitude of the second effect, that of shearing the reduced sections rearward to the angle Λ. Examination of the curves reveals that the effect of the t/c reduction in the free-stream direction contributes from approximately 40 to 55 percent the total C_{D_W} reduction due to sweepback. Thus, the advantage of sweepback in the manner described above is seen to lie partly in the effect of creating thinner airfoil sections in the free-stream direction.

Wing Section Profile

In figure 11 are shown the curves of C_{D_T} against M for winged configurations having 45° sweptback wings of diamond and circular-arc

[redacted]

profiles. Also included are the rectangular-wing configurations for the NACA 65-009 and circular-arc airfoil sections from reference 2 and the swept-wing configuration with NACA 65-009 airfoil section from reference 3. The wingless configuration, discussed in the preceding section, is here based on a wing area of 1.389 square feet. All winged configurations had wings of equal exposed plan-form area and 2.7 aspect ratio. The sections were all 9 percent thick in planes normal to the wing leading edges. Lack of sufficient data prevented the inclusion of a configuration with rectangular wings of diamond section. C_{D_W} for the above configurations is presented in figure 12 against M. The curves indicate that, whereas airfoil section has a marked effect on the drag coefficient of an unswept wing, it has but little effect for a 45° sweptback wing. In both the swept and unswept plan form, the wing with NACA 65-009 airfoil sections shows somewhat less C_{D_W} than do the sharp-nose airfoils. This condition may, however, be reversed at higher Mach numbers where the shock will attach itself to the nose of the sharp-nose airfoils.

CONCLUSIONS

Flight tests were conducted on airplane-like configurations to determine the effect on drag of wing section profile and thickness ratio. The Mach number range of the tests was approximately 0.95 to 1.3 corresponding to an average Reynolds number range from approximately 5×10^6 to 9×10^6. Within the scope of the tests, the following effects on drag were notable:

1. A decrease in thickness ratio resulted in a marked reduction of wing drag.

2. Over the thickness range investigated, the reduction of drag with decreasing thickness was less rapid for the round-nose airfoils than indicated by the theoretical thickness-squared relation for supersonic flow.

3. Almost half the drag reduction, due to sweepback, resulted from the decrease of the section thickness ratio in the free-stream direction.

4. Although sharp-nose profiles showed greater drag for the rectangular wings than did the NACA 65-009 airfoil section profile, the

difference was very small for the 45° sweptback wings. However, the sharp-nose airfoils may show lower drag at higher Mach numbers where the nose wave is attached.

Langley Memorial Aeronautical Laboratory
National Advisory Committee for Aeronautics
Langley Field, Va.

REFERENCES

1. Ferri, Antonio: Experimental Results with Airfoils Tested in the High-Speed Tunnel at Guidonia. NACA TM No. 946, 1940.

2. Alexander, Sidney R.: Drag Measurements of Symmetrical Circular-Arc and NACA 65-009 Rectangular Airfoils Having an Aspect Ratio of 2.7 as Determined by Flight Tests at Supersonic Speeds. NACA RM No. L6J14, 1946.

3. Tucker, Warren A., and Nelson, Robert L.: Drag Characteristics of Rectangular and Swept-Back NACA 65-009 Airfoils Having Various Aspect Ratios as Determined by Flight Tests at Supersonic Speeds. NACA RM No. L7C05, 1947.

4. Alexander, Sidney R., and Katz, Ellis: Flight Tests to Determine the Effect of Length of a Conical Windshield on the Drag of a Bluff Body at Supersonic Speeds. NACA RM No. L6J16a, 1947.

5. von Kármán, Th.: Turbulence and Skin Friction. Jour. Aero. Sci., vol. 1, no. 1, Jan. 1934, pp. 1-20.

6. Bonney, E. Arthur: Aerodynamic Characteristics of Rectangular Wings at Supersonic Speeds. Jour. Aero. Sci., vol. 14, no. 2, Feb. 1947, pp. 110-116.

[redacted]

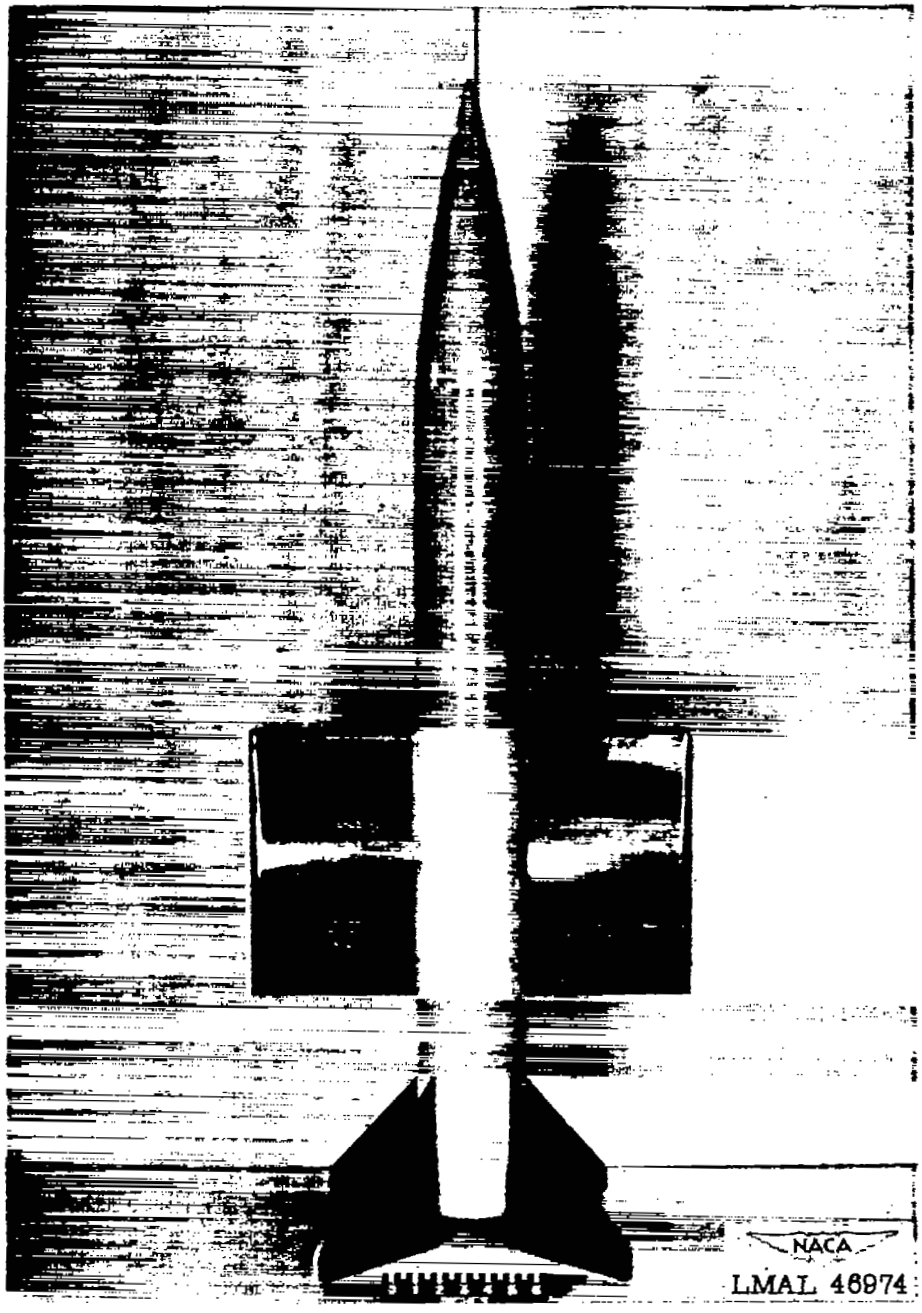

Figure 1.- Typical configuration used in thickness-ratio investigation.

NATIONAL ADVISORY COMMITTEE FOR AERONAUTICS
LANGLEY MEMORIAL AERONAUTICAL LABORATORY - LANGLEY FIELD, VA

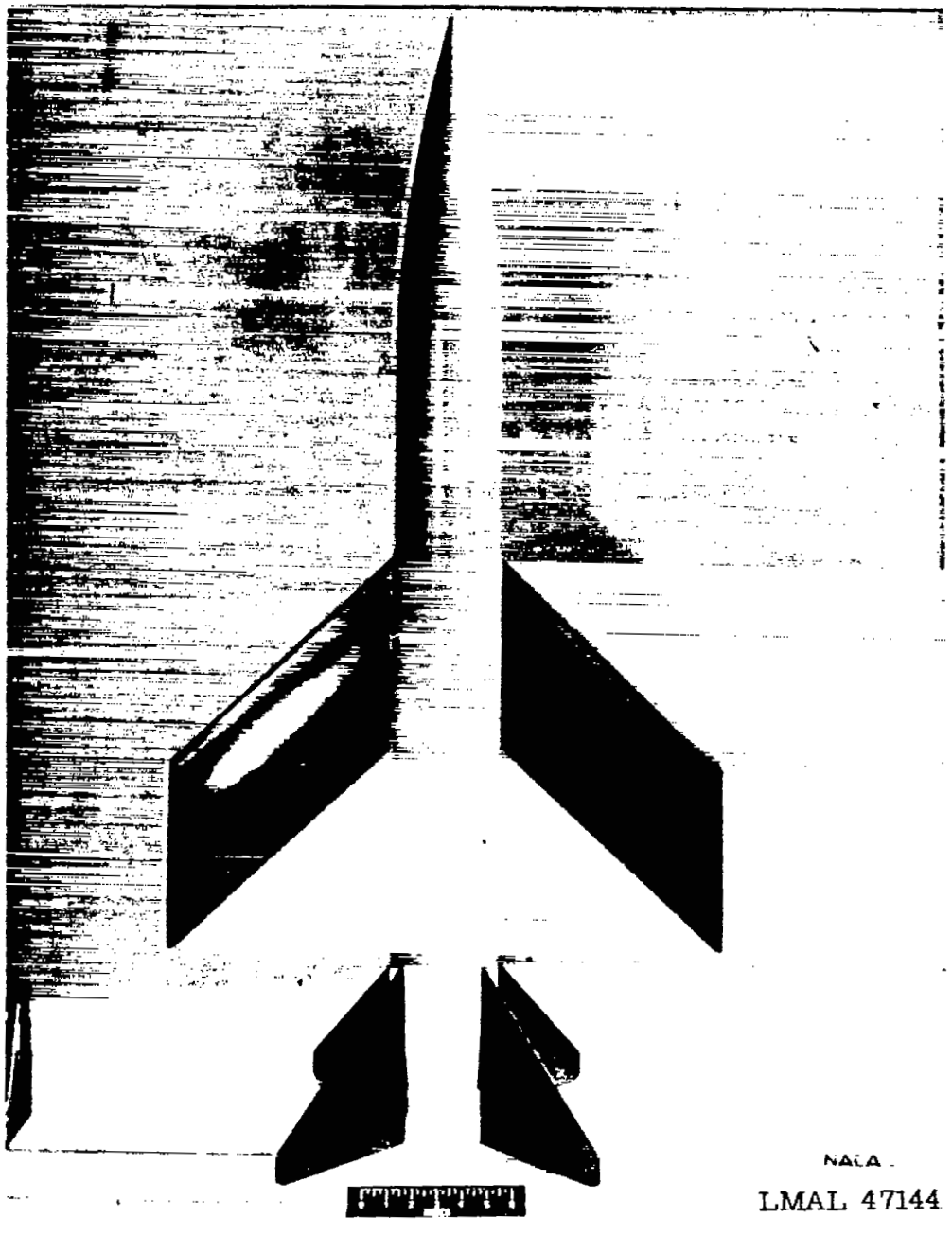

Figure 2.- Typical configuration used in section profile investigation.

NATIONAL ADVISORY COMMITTEE FOR AERONAUTICS
LANGLEY MEMORIAL AERONAUTICAL LABORATORY - LANGLEY FIELD VA

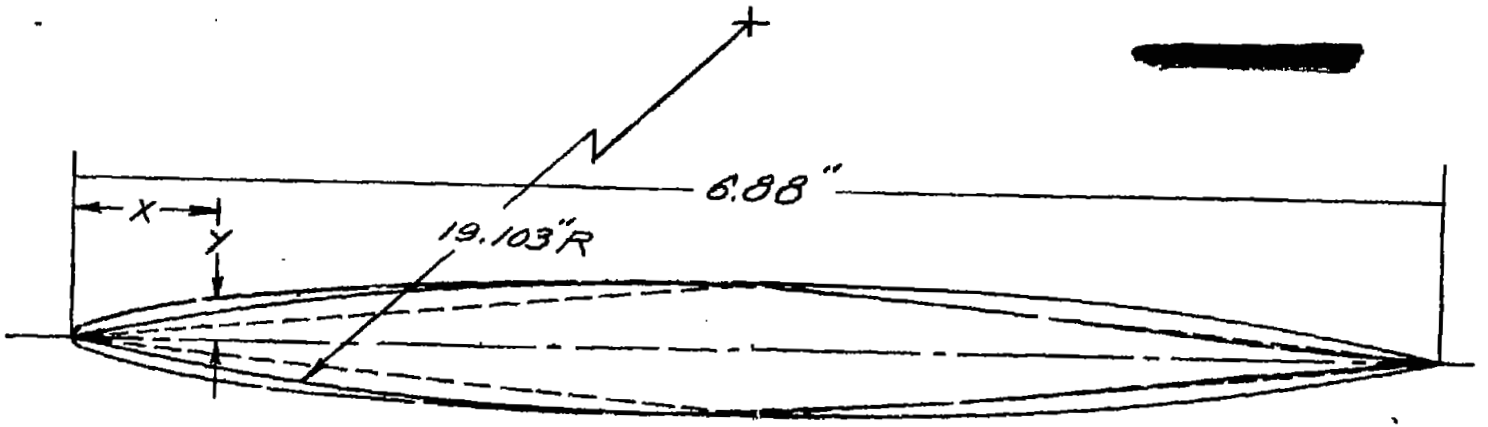

NACA 65-009 airfoil coordinates in percent chord			
X	Y	X	Y
0	0	40	4.496
0.5	.700	45	4.469
0.75	.845	50	4.336
1.25	1.058	55	4.086
2.5	1.421	60	3.743
5.0	1.961	65	3.328
7.5	2.383	70	2.856
10	2.736	75	2.342
15	3.299	80	1.805
20	3.727	85	1.260
25	4.050	90	.738
30	4.282	95	.280
55	4.431	100	0
Leading-edge radius; 0.552			

Circular-arc

NACA 65-009

Diamond

Figure 3. - Comparison of NACA 65-009, circular-arc, and diamond sections for 45° sweptback wings. Sections taken normal to leading edge.

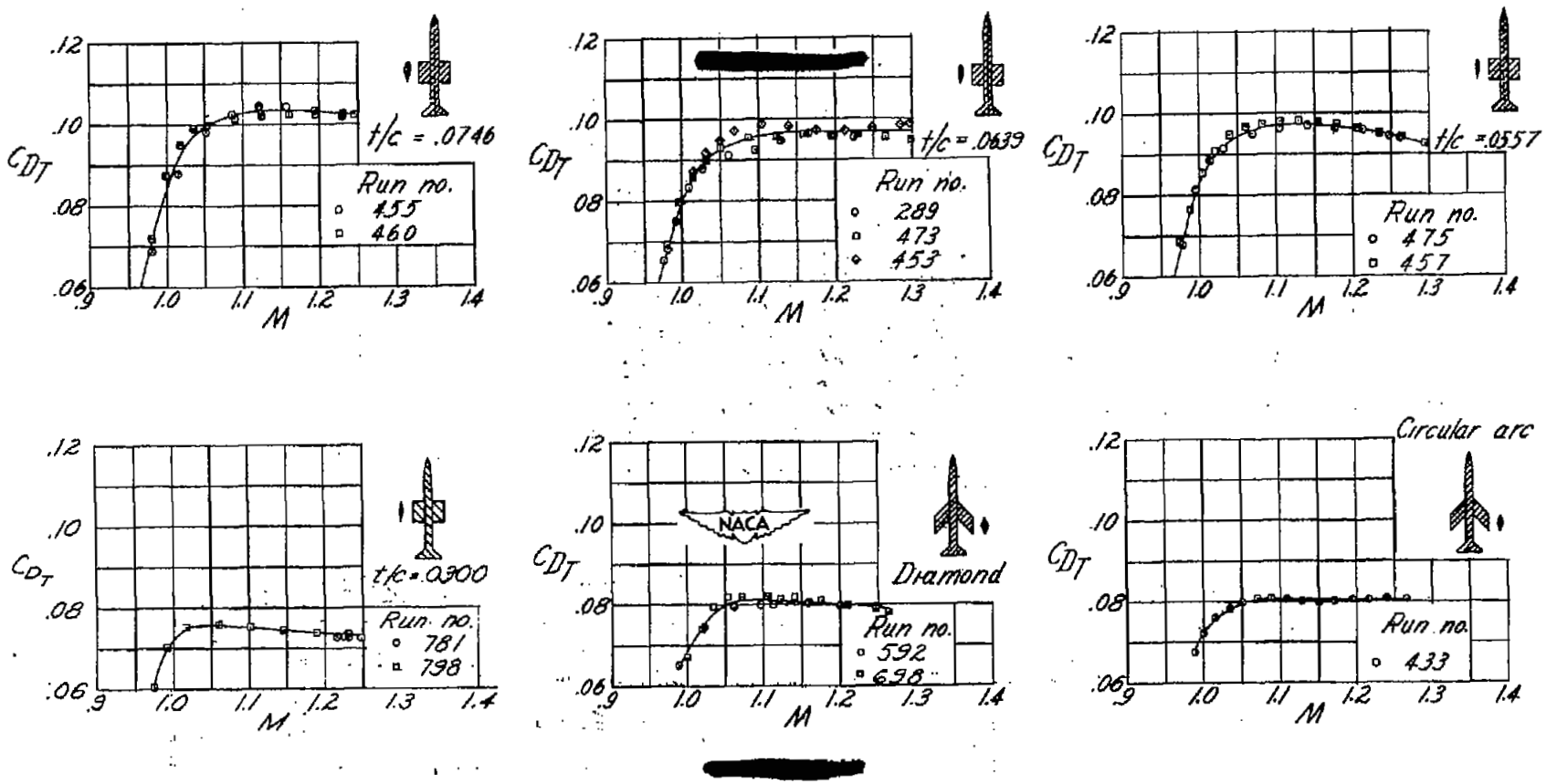

Figure 4.- Basic data for the models of each configuration tested.

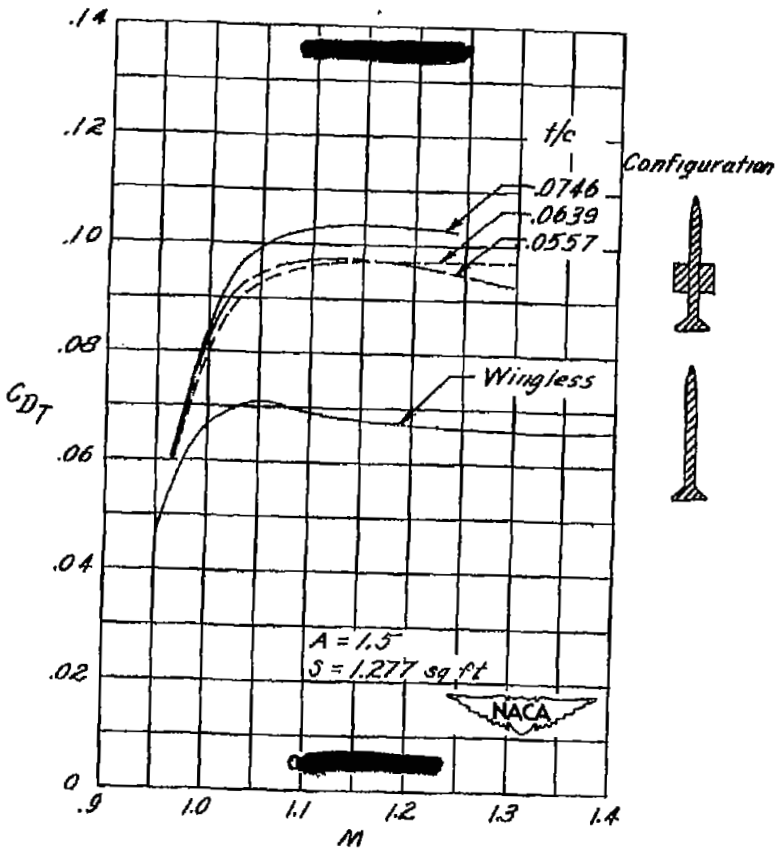

Figure 5.- Curves of C_{D_T} for configurations having rectangular wings of NACA 65-series sections for t/c =0.0746, 0.0639, and 0.0557.

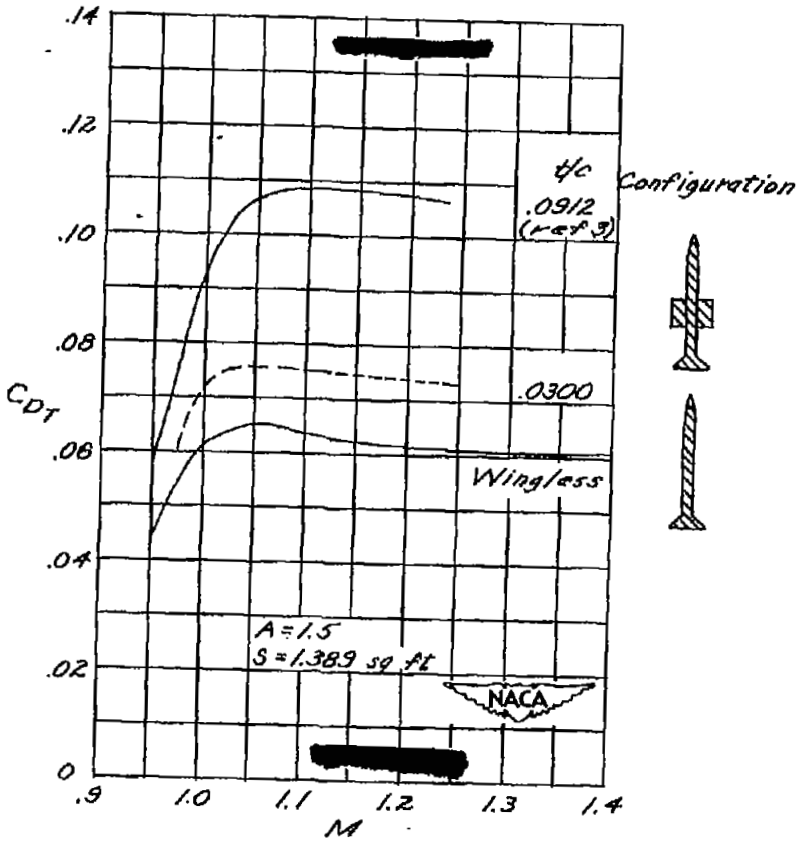

Figure 6.- Curves of C_{D_T} for configurations having rectangular wings of NACA 65-series sections for t/c =0.0912 and 0.0300.

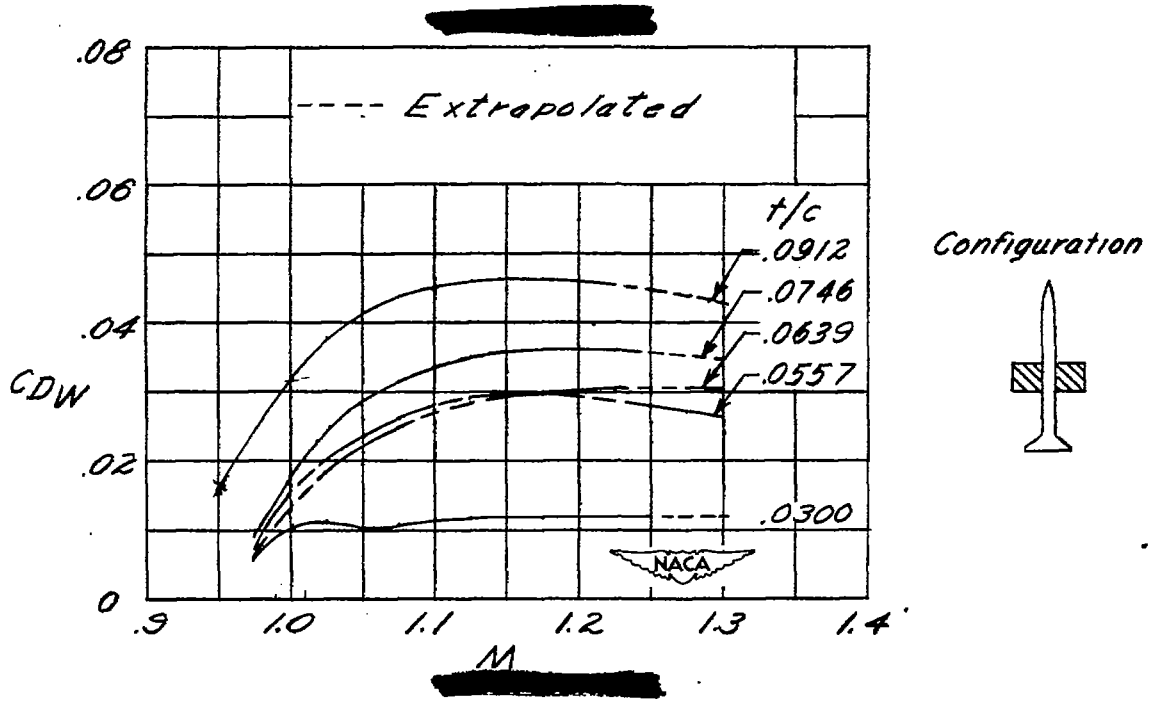

Figure 7.- Curves of C_{DW} for rectangular wings of NACA 65-series sections for four thickness ratios. A = 1.5.

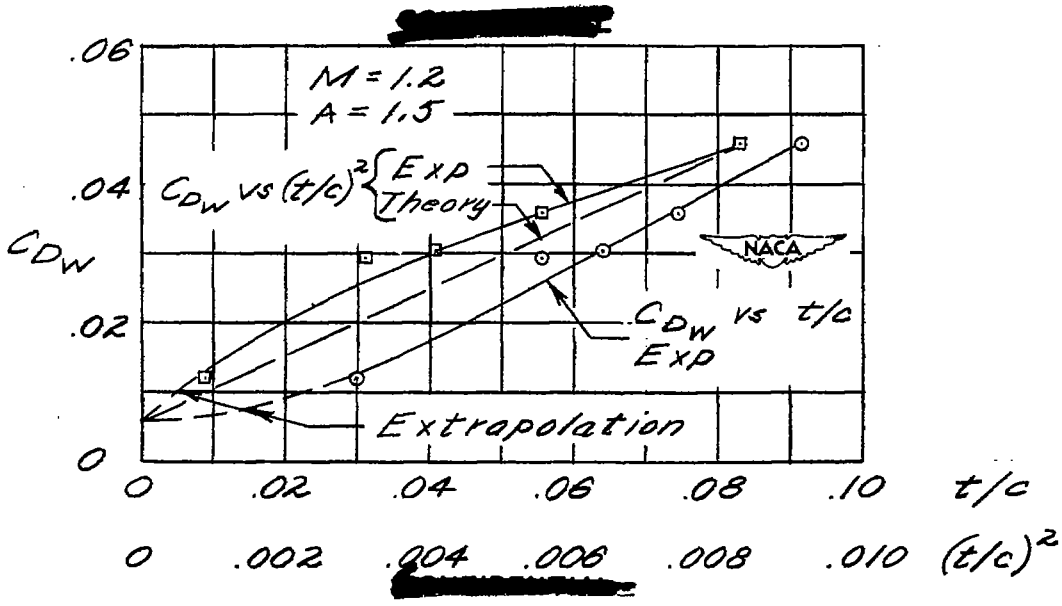

Figure 8.- Variation of C_{DW} with t/c and $(t/c)^2$ for rectangular wings having 65-series sections; comparison of experiment with supersonic theory.

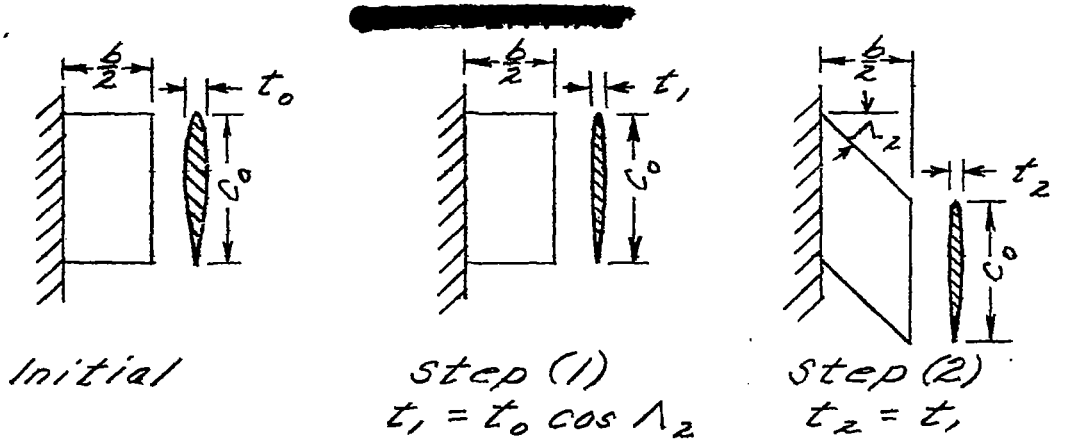

Figure 9.- Steps taken in sweeping a wing to Λ. $b/2$, c_0 = constant.

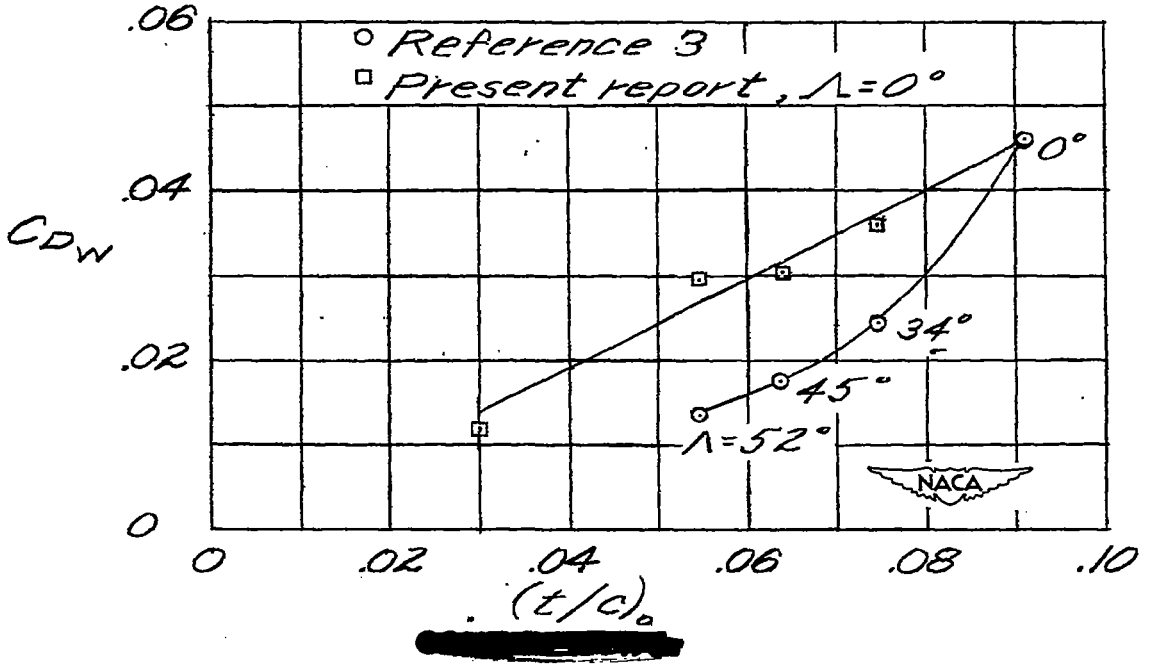

Figure 10 - Variation of C_{D_W} with free stream t/c for swept and unswept wings; M = 1.2. Upper curve is effect of step (1) of figure 9 and lower curve is effect of steps (1) and (2).

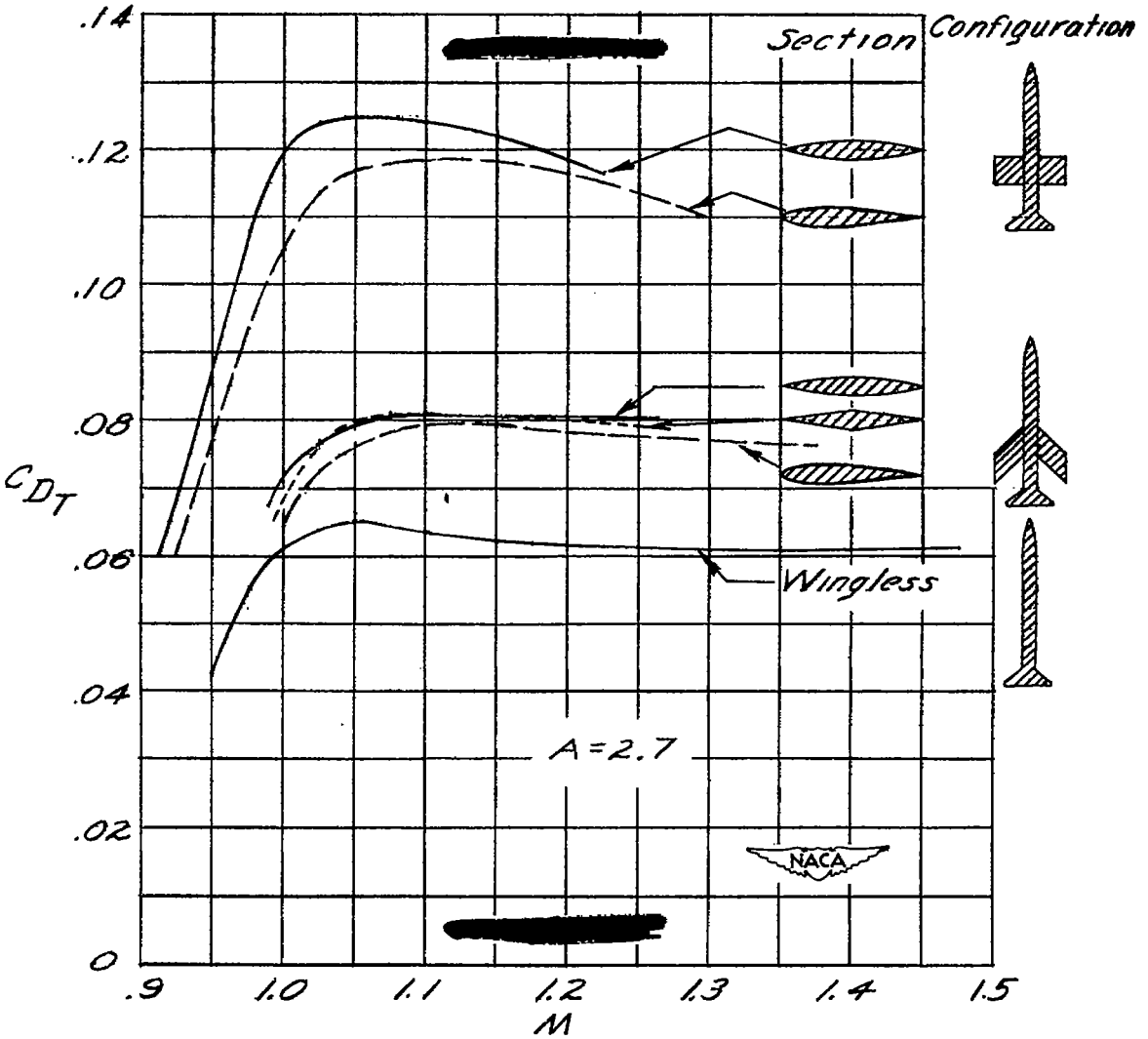

Figure 11. - Curves of C_{D_T} for the NACA 65-009, circular-arc, and diamond section airfoil configurations; $\Lambda = 0°$ and 45°.

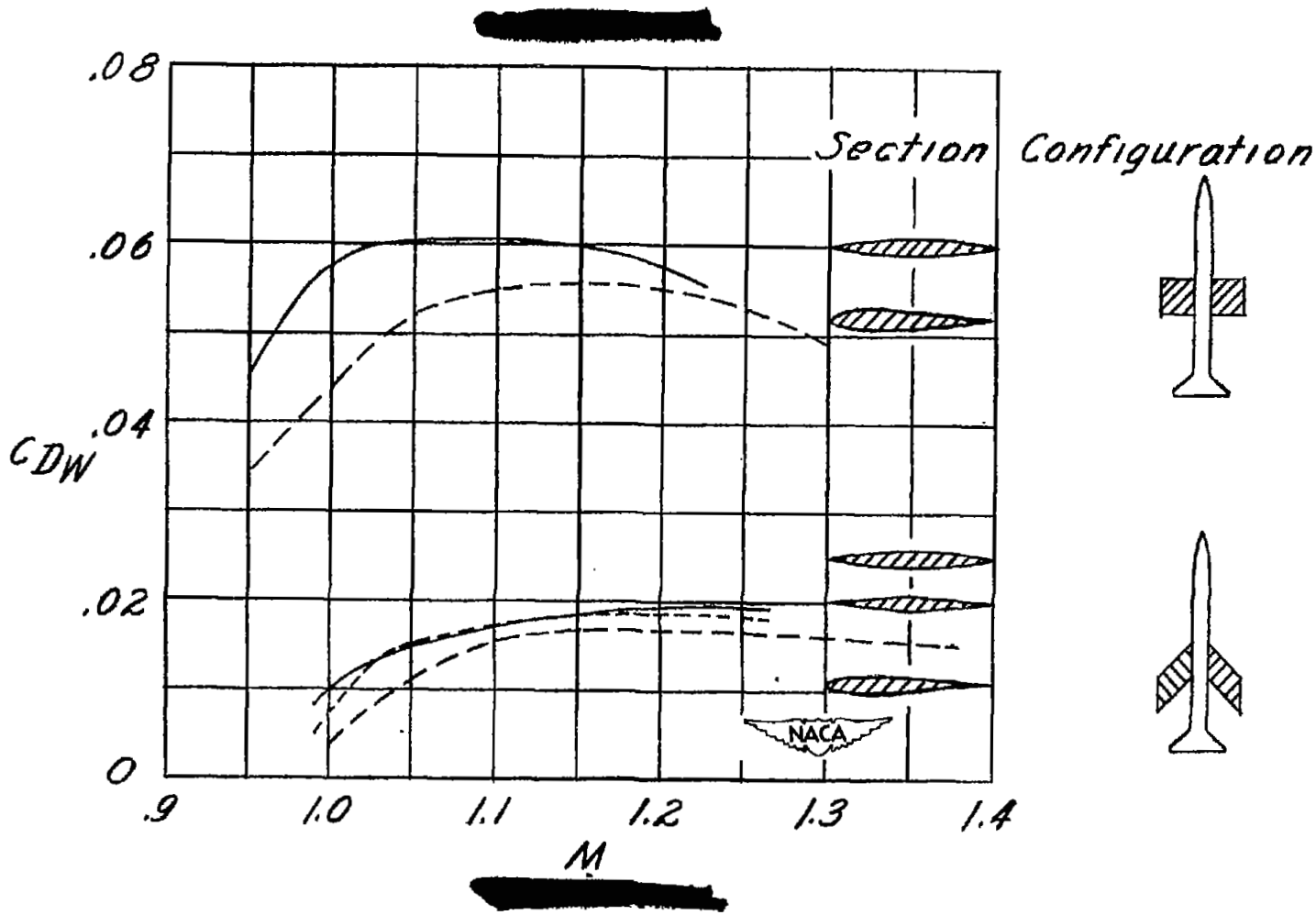

Figure 12.-Curves of C_{DW} for the NACA 65-009, circular-arc, and diamond section airfoil configurations; $\Lambda = 0°$ and $45°$. $A = 2.7$.